EurJOC
European Journal of Organic Chemistry

Research Article
doi.org/10.1002/ejoc.202200769

Chemistry Europe
European Chemical Societies Publishing

www.eurjoc.org

Benzo[*c*][1,2]thiazine-Based Analogs in the Inverse Electron Demand [4+2] Hetero Diels-Alder Reaction with Glycals: Access to Tetracyclic Fused Galactose and Fucose Derivatives

Giacomo Biagiotti,[a] Laura Legnani,[b, c] Giusi Aresta,[a] Maria A. Chiacchio,[c] and Barbara Richichi*[a]

In memory of Prof. Giovanni Romeo, who gave a fundamental contribution to the field of cycloaddition reactions

The synthesis and reactivity in an [4+2] inverse electron demand hetero Diels-Alder reaction (ihDA) of an original class of electron-poor heterodienes, the *N*-substituted-1H-benzo[c][1,2]thiazin-4-one-2,2-dioxides, are described. These are highly reactive electrophiles that allow easy access to unprecedented benzo-thiazine glyco-fused derivatives in a remarkably selective way, even when using acetylated glycals, previously unexplored within this version of ihDA. DFT calculations support the experimental data, and moreover show that acetylated dienophiles can easily react making cycloadditions feasible.

Introduction

Glycomimetics have proven to be useful tools in tackling fundamental questions in glycobiology and provide cutting-edge therapeutic strategies that address current unmet needs in diverse disease settings.[1] The advantages of glycomimetics rely on their ability to mimic the structural and functional information of native carbohydrates, allowing for the fine tuning of sugar-encoded information. Improved drug-like properties, enzymatic stability and pre-organized bioactive conformations afford glycomimetics vast therapeutic potential and thus allow them to overcome many of the inherent limits of their natural counterparts that make them poor choice as therapeutics.[2] Presently, they comprise a major share within the drug development market and Oseltamivir,[3] Zanamivir,[4] Voglibose,[5] Miglitol,[6] Miglustat,[7] Topiramate,[8] Gliflozins[9] and a few other *C*-glycosides[10] are just some of currently approved glycomimetic drugs. With the aim of speeding up the discovery of drugs able to modulate glycan-based recognition events, much effort has been devoted toward the identification of straightforward methodologies to produce glycomimetic architectures with a broad structural diversity.[11]

In this framework, the contribution of some of us came from a synthetic approach that allowed for the preparation of an array of glycomimetics in a highly selective way. This process relies on an original version of an [4+2] inverse electron demand hetero Diels-Alder reaction (ihDA) that involves structurally different oxothiones and *o*-thioquinones as electron-poor heterodienes and protected glycals as electron-rich dienophiles.[12] This approach afforded bi- and tricyclic architectures bearing a glycofused 1,4-oxathiin ring (*i.e.* compounds **1**–**4**, Figure 1).[13] The molecular mimicry properties of these molecules allowed for the investigation of the biological effect that these glycomimetics had in specific contexts where the

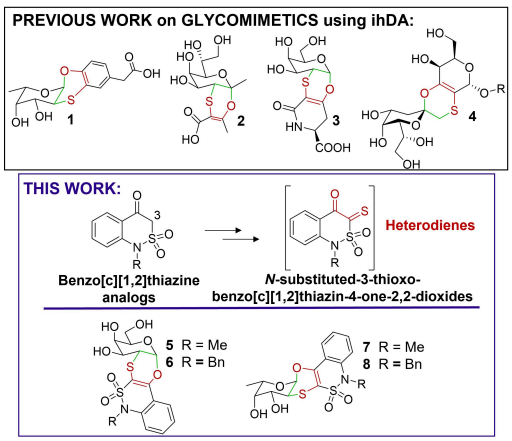

Figure 1. Structures of mimetics of fucose **1**,[12a] KDO **2**,[12b] Tn-antigen **3**,[12c] and GM3-lactone **4**[12d] prepared so far by ihDA. General structures of benzo[c][1,2]thiazine-based analogs, structure of the *N*-substituted-1H-benzo[c][1,2]thiazin-4-one-2,2-dioxides and of the galactose and fucose derivatives **5**–**8** described in this work.

[a] *Dr. G. Biagiotti, G. Aresta, Prof. B. Richichi*
Department of Chemistry "Ugo Schiff", University of Firenze
Via della Lastruccia 13, 50019, Sesto Fiorentino, FI, Italy
E-mail: barbara.richichi@unifi.it
[b] *Dr. L. Legnani*
Department of Biotechnology and Bioscience,
University of Milano-Bicocca
Piazza della Scienza 2, 20126 Milano, Italy
[c] *Dr. L. Legnani, Prof. M. A. Chiacchio*
Department of Pharmaceutical and Health Sciences, University of Catania
Viale A. Doria 6, 95125 Catania, Italy

Supporting information for this article is available on the WWW under https://doi.org/10.1002/ejoc.202200769

Research Article
doi.org/10.1002/ejoc.202200769

recognition of carbohydrates plays a crucial role leading to the identification of antibacterial agents[13a,14] (compound **1**, Figure 1) inhibitors of glycosyltransferases[15] and glycosidases[13b] (compounds **1**–**2**, Figure 1), and tumor associated carbohydrate antigens[16–19] (compounds **3**–**4**, Figure 1).

Therefore, we demonstrated the versatility of this strategy in tackling the challenge of providing structural diversity by means of utilizing readily accessible protected glycals and modular heterodienes.

In this framework, we report here the synthesis of a new class of electron-poor heterodienes the *N*-substituted-1H-benzo[c][1,2]thiazin-4-one-2,2-dioxides (Figure 1). Then, we have investigated the reactivity of the heterodienes in the context of an ihDA reaction using L-fucal and D-galactal as model glycals. This approach allows easily accessing to unprecedented four new tetracyclic galactose and fucose derivatives (compounds **5**–**8**, Figure 1) bearing different *N*-substituted 1,2-benzothiazine rings. Then, the reaction mechanisms, involving the *N*-methyl-1H-benzo[c][1,2]thiazin-4-one-2,2-dioxide, were studied through DFT calculations.

Results and Discussion

Synthesis of the N-substituted-3-thioxo-benzo[c][1,2]thiazin-4-one-2,2-dioxides and of the galactose and fucose derivatives 5–8

A few previous works described that *N*-substituted-1*H*-benzo[c][1,2]thiazin-4-one-2,2-dioxides (Figure 1) react with electrophiles providing adducts with diverse substituents in position C-3.[20,21] On this basis, we investigated the nucleophilicity of position C-3 of the benzo[c][1,2]thiazine-based analogs **9** and **10**,[22] bearing respectively a *N*-methyl and *N*-benzyl substituents, in the reaction with the phthalimidesulfenyl chloride **11** (Scheme 1).[23]

Compound **11** is a well-known sulphenylating agent bearing an electrophilic sulfur atom that proved to quickly react with a wide group of electron rich arenes and enolizable carbonyl derivatives and affording *o*-hydroxythiophthalimide and α-α′-dioxothiophthalimide derivatives respectively.[23,12a] In turn, in this work, the synthesis of the *N*-thiophthalimides **12** and **13** (Scheme 1) was accomplished by the addition of freshly prepared **11** to a solution of **9** and **10** respectively, in mild conditions ($CHCl_3$, rt, 1 h). Pure *N*-thiophthalimides **12** and **13** were obtained in high yield (75% for **12**, 79% for **13**) and were stored for more than 2 years at 4 °C proving to be stable compounds. Both *N*-thiophthalimides **12** and **13** were in a keto:enol tautomeric mixtures in a 1:5.5 and 1:1.7 ratio respectively, as revealed by ^{1}H-NMR spectra (peak integration of the O–H signal (enol) at 10.1 ppm and of the H-3 signal (ketone) at 4.34 ppm for **12** and 4.24 ppm for **13**, see Supporting Information). *N*-Thiophthalimides **12** and **13** are precursors of the corresponding *N*-substituted-3-thioxo-benzo[c][1,2]thiazin-4-one-2,2-dioxides **14** and **15** (Scheme 2) which are readily prepared by deprotonation with a weak base (*i.e.* pyridine) of the acidic proton in position C-3.

In turn, thiones **14** and **15** are highly reactive species, and they were trapped *in situ* with electron-rich 4,6-*O*-di-*tert*-butylsilylidene D-galactal **16**[24] and the 3,4-*O*-di-*tert*-butylsilylidene L-fucal **17**[13a] (Scheme 2) in a totally selective ihDA route affording the corresponding cycloadducts **18**–**21** bearing the 1,4-oxathiin ring. Cycloaddition reactions were monitored by ^{1}H-NMR spectroscopy (Figure S1–S2, Table S1) over time (t = 0–48 h) by following the disappearance over time of the signals of the olefin protons at 6.30 ppm (H-1 signal) and 4.71 ppm (H-2 signal) for D-galactal **16** (Figure S1A), and at 6.38 ppm (H-1 signal) and 4.74 ppm (H-2 signal) for L-fucal **17** (Figure S2A) respectively. The formation of the galactose (Gal) derivatives **18** and **19** and of the fucose (Fuc) derivatives **20** and **21** was monitored by following the appearance of the signals at 5.89/5.81 ppm (H-1 signal) and 3.61 ppm (H-2 signal) of **18** and **19** (Gal series, Figure S1B–S1C), and at 5.90/5.82 ppm (H-1 signal) and 3.69 ppm (H-2 signal) of **20** and **21** (Fuc series, Figure S2B–S2C) respectively.

Cycloaddition reactions with silylated glycals (both Gal/Fuc) proceeded smoothly using an excess of the *N*-thiophthalimides **12** or **13** (up to two equivalents were added overtime as separate batches, see experimental). After 48 h all reactions were almost complete (Figure S1–S2). Only the ihDA between **17** (Fuc series) and the *N*-thiophthalimide **12** proceed slowly (**17**, 6.38 ppm, H-1 signal, < 23% residual peak, Figure S2) whereas a residual peak < 3% at 6.30 ppm (**16**, H-1 signal,

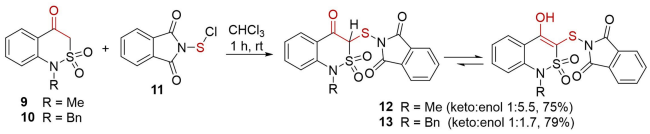

Scheme 1. Synthesis of the *N*-thiophthalimides **12** and **13.**

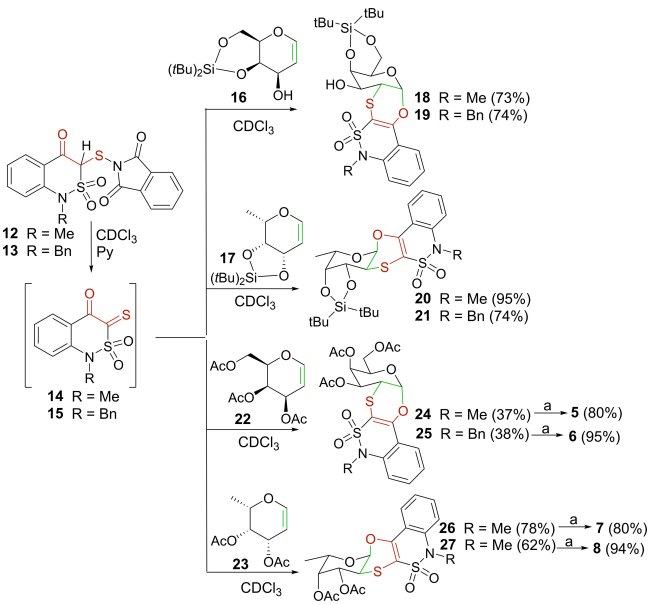

Scheme 2. Synthesis of the cycloadducts **18**–**21** and **24**–**27**. Reaction conditions: a) K_2CO_3, MeOH, 1 h, r.t.

Research Article
doi.org/10.1002/ejoc.202200769

Figure S1) for the Gal series was observed. Then, cycloadducts **18**–**21** were isolated, by flash chromatography on silica gel column, in high yields (73% for **18**, 74% for **19**, 95% for **20**, 74% for **21**). ^{1}H NMR analysis allowed the determination of the structures of the cycloadducts **18**–**21**. As expected,[12a,13a,24] ihDA reactions with both silylated glycals **16** and **17** were totally regio- and stereoselective. The chemical shift of the H-1 and H-2 signals of cycloadducts **18**–**19** (Gal series, Figure S1B–S1C) and **20**–**21** (Fuc series, Figure S2B–S2C) confirmed that the sulfur of the diene reacts with the C-2 of the glycals. In particular, as previously described,[13a,c,24] the H-2 signals of **18**–**21** are in a range of chemical shift (3.6–3.7 ppm) that is compatible with the presence of a sulfur atom linked to the C-2. The axial-axial coupling constants of the doublet of doublet of the H-2 signals ($J_{2\text{-}3}$ = 10.6 Hz for **18**–**19** and $J_{2\text{-}3}$ = 10.9 Hz for **20**–**21**) confirmed that the cycloadducts obtained by the selective attack to the less hindered face of the corresponding glycals (*i.e.* bottom face of D-galactal **16** and top face of L-fucal **17**) were obtained.[13a,c]

Then, in this work, we decided to investigate, for the first time, the reactivity in ihDA reactions of both D-galactal and L-fucal protected with acetyl groups. Glycals are often prepared starting from the corresponding peracetylated monosaccharides.[25,26] Therefore, the possibility to use acetylated glycals in ihDA reactions would allow for the creation of glycomimetics in a straightforward way by avoiding the manipulation of the acetylated glycals with time-consuming protection-deprotection steps. Indeed, the selection of the proper protective group is not trivial[12b] as the compatibility with the double bond in the glycals and the sulphur atom of the oxathiin ring in the products significantly limit our options. In addition, in some cases, further acetylation of the cycloadduct is an additional step required for the exhaustive purification of the cycloadduct after the removal of the temporary protective group.[13a] Therefore, *N*-thiophthalimides **12** and **13** were reacted with 2,3,6-triacetyl-galactal **22** and 2,3-diacetyl-fucal **23** (Scheme 2). Cycloaddition reactions were monitored by ^{1}H-NMR spectroscopy (Figure S3–S4, Table S1) by following the disappearance over time of the signals of the olefin protons at 6.42 ppm (H-1 signal) and 5.50 ppm (H-2 signal) for D-galactal **22** (Figure S3A), and at 6.46 ppm (H-1 signal) and 5.55 ppm (H-2 signal) for L-fucal **23** (Figure S4A) respectively. As expected, ihDA reactions with acetylated D-galactal **22** proceeded slower (Figure S3–S4, see Supporting Information). Neither the addition of an excess of the *N*-thiophthalimides **12** and **13** (up to 3.6 equivalents) or longer reaction times (up to 192 h) allowed for a complete conversion of **22** into the corresponding cycloadducts **24**–**25** (Figure S3, see Supporting Information). In addition, after 144 h the reaction mixture became reddish, a potential indicator of decomposition, and cycloadducts **24**–**25** were only isolated in moderate yields (37% for **24**, 38% for **25**). Conversely, acetylated fucal **23** showed a remarkably higher reactivity in the same experimental conditions. After 72 h ihDA reactions were completed (Figure S4, see Supporting Information) and cycloadducts **26**–**27** were isolated in high and good yields (78% for **26**, 62% for **27**). Finally, cycloadducts **24**–**27** were deprotected (Scheme 2) using mild basic conditions (K_2CO_3, MeOH) thus affording the corresponding compounds **5**–**8** in high yields (80–95%).

Molecular modeling

Relying on these data we sought to further investigate by comparing the observed reactivity of both couples of differently protected dienophiles silylated **16**–**17** and acetylated **22**–**23** glycals with this original class of heterodienes using the B3LYP[7] density functional approach.[27] The regioselectivity of this type of ihDA has been previously investigated by some of us, limiting the study to simplified model dienes/dienophiles.[28]

In this work, both silylated and acetylated glycals were considered as experimental reactants, to provide insights, from a stereoelectronic perspective, on the observed reactivity of acetylated glycals in the ihDA route. Then, compound **14** was directly selected as a diene and optimized. According to the electronic effects of the ihDA mechanism, the dominant electronic interaction between the $HOMO_{dienophile}$ and the $LUMO_{diene}$,[29] was further confirmed by the energy values of the LUMO/HOMO orbitals of compounds **14**,**16**–**17**,**22**–**23** (Table 1).

Diene **14** is completely planar ($\tau_{(O=C-C=S)} = 0$) with the carbonyl and thiocarbonyl moieties properly oriented for the ihDA (Figure S5). It can be ascribed as among the most reactive dienes (strong electrophile) described so far ($E_{LUMO} = -4.38$),[28] as confirmed by the electrophilicity index (Ω) (6.45 eV, Table 1). In accordance with experimental data, the difference (ΔE) between $LUMO_{diene}$ and $HOMO_{dienophile}$ follows the order **17** < **16**, **23** < **22** (Table 1).

Silylated dienophiles **16** and **17** are conformationally blocked whereas acetylated dienophiles **22** and **23** show a certain degree of conformational freedom, due to the presence of the acetyl groups. So, in order to study the cycloaddition reaction of acetylated glycals, all the degrees of conformational freedom of **22** and **23** were preliminarily considered, focusing on the orientation of the acetyl groups (Figure 2). They are described by the torsional angles τ_1 [C(2)–C(3)–O–C(3′)], τ_2 [C(5)–C(4)–O–C(4′)], τ_3 [O–C(5)–C(5′)–C(O)], and τ_4 [C(5)–C(5′)–C(O)–C] in **22**, and τ_1 [C(1)–C(6)–C(7)–C(8)] and τ_2 [C(7)–C(8)–C(9)–C(10)] in **23** (Figure 2, Table 2).

Once the preferred geometries of the reactants were determined, we located the transition states leading to cycloadducts **18**, **20**, **24** and **26**, considering the alternative *endo*/*exo* arrangements of dienophiles **16**, **17**, **22**, **23** with respect to the

Table 1. Computed data of the minimum energy conformation of diene **14** and dienophiles **16–17**, **22–23**. Ω[30] = electrophilicity index, N = nucleophilicity index.[31,32]

Compounds	E_{HOMO} [eV]	E_{LUMO} [eV]	Ω	N	ΔE ($LUMO_{diene}$ – $HOMO_{dienophile}$)
14	−6.81	−4.38	6.45	4.35	–
16	−6.46	−0.39	0.97	4.70	2.07
17	−6.36	−0.25	0.89	4.80	1.97
22	−6.70	−0.38	0.99	4.46	2.32
23	−6.51	−0.29	0.93	4.65	2.13

Research Article
doi.org/10.1002/ejoc.202200769

Chemistry Europe
European Chemical Societies Publishing

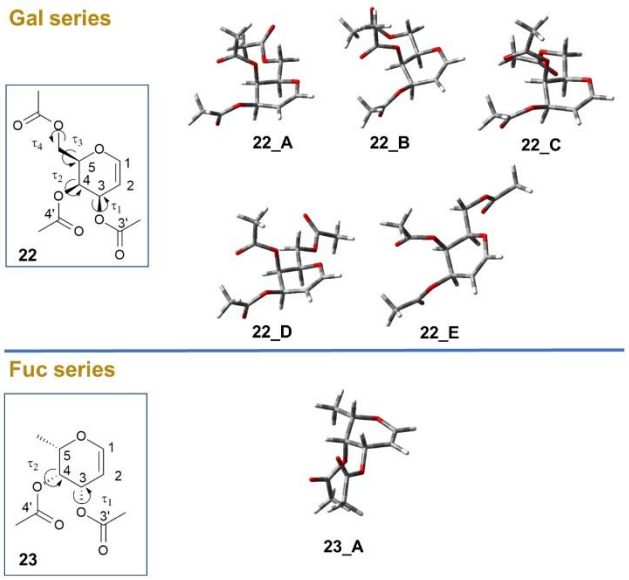

Figure 2. Degrees of conformational freedom of acetylated dienophiles **22** and **23** and 3D plots of the located conformations of acetylated D-galactal **22** (**A**–**E**) and acetylated L-fucal **23 A**.

Table 2. Relative energies, equilibrium percentages and main geometrical data of the conformations of compounds **22** and **23**.

	ΔE [kcal/mol]	%	τ_1[x]	τ_2[y]	τ_3[z]	τ_4[m]	ΔG [kcal/mol]	%
22 A	0.00	55	−146	145	172	174	0.00	45
22 B	0.20	39	−147	140	174	129	0.64	16
22 C	0.40	28	−148	146	178	−86	0.84	11
22 D	0.70	17	−146	145	70	−172	0.44	22
22 E	0.88	12	−144	146	63	82	1.20	6
23 A	0.00	100	146	−144	/	/	0.00	100

[x] τ_1: [C(2)–C(3)–O–C(3′)]; [y] τ_2: [C(5)–C(4)–O–C(4′)]; [z] τ_3: [O–C(5)–C(5′)–C(O)]; [m] τ_4: [C(5)–C(5′)–C(O)–C] in **22**, and τ_1 [C(1)–C(6)–C(7)–C(8)] and τ_2 [C(7)–C(8)–C(9)–C(10)] in **23**.

diene **14** and the two possible approaches of **14** to the double bond of the dienophiles (over or under) (Figure 3). The orientations of the acetyl groups in the preferred conformations **22 A** and **23 A** (Table 2), respectively, were selected for the optimizations of the transition states.

In Figure 3 the 3-D plots of the most stable transition states located for the different reactions are highlighted (*i.e.* TS18u*x*, TS24u*x*, TS20o*x*, TS26o*n*), with the bond forming distances reported (Å). In all the TSs both the C–S and C–O bonds are in formation, but the processes are not synchronous as shown by values of $\Delta d_{TS/P}$ (Table S2), ranged, for the favorite reaction channels, from 0.18 to 0.32.

IRC analysis confirmed that the reaction is concerted, albeit asynchronous, reaching the reaction products in the forward direction and the cycloaddends in reverse, without evidence of any intermediate structure along the reaction paths. The two addends pass through a bimolecular complex (Figure 3) with a nonbonding interaction between the sulfur atom of diene and the double bond of dienophiles. These complexes in the cases of dienophiles **17**, **22**, **23** are minima located in the energy profiles, but not in the free energy ones (Figure 4, Figures S6–S8).

As representative example, Figure 4 shows the energy (A) and free-energy (B) profiles determined for the favorite channel of reaction of **14** with **23**, showing the high feasibility of the cycloaddition involving the acetylated L-fucal **23**. Notably, the presence of either the silyl or the acetyl protective groups of glycals did not matter, as the energy and free energy activation barriers were low in all the considered ihDA, as highlighted by $\Delta E^{\neq}$ and $\Delta G^{\neq}$ values reported in Table S2, thus revealing that all the reactions are allowed. These results confirm the possibility to produce these fucose derivatives using more affordable acetylated dienophiles.

Conclusion

In summary, we reported the synthesis of an unique class of highly reactive *N*-substituted-3-thioxo-benzo[c][1,2]thiazin-4-one-2,2-dioxides. These heterodienes allow for the assembly of four novel galactose and fucose derivatives bearing an unprecedented benzo-thiazine fused moiety. They were prepared in a straightforward way that implies the use of acetylated glycals as dienophiles. Computational mechanistic studies confirm the low energy barriers necessary for cycloaddition reactions involving this class of compounds. Additional studies are currently underway to further investigate ihDA for the incorporation of other acetylated glycals and structurally different heterodienes allowing the manufacture of glyco-fused architectures bearing the 1,4-oxathiin ring, while avoiding protection-deprotection steps. Of note, owing to the growing range of biological implications of glycomimetics and the emerging role of benzo-thiazine in the panorama of drug discovery,[33] this study could make available a new generation of glycomimetic drugs.

Experimental Section

Materials and methods

All reagents and solvents were purchased from Sigma-Aldrich and they have been used without any further purification, if not specified otherwise. Flash chromatography was performed on Merk silica gel 60 (0.040–0.063 mm). Thin layer chromatography was performed on Supelco TLC Silica gel 60 F_{254} (aluminium sheets or glass plates). FT-IR spectra were recorded on IRAffinity-1S spectrometer, and the data were collected and elaborated with Lab Solution IR v. 2.16 software. NMR spectra were recorded on Varian Inova 400, Mercury plus 400 and Gemini 200 instruments. Chemical shifts were reported in parts per million (ppm) relative to the residual solvent peak rounded to the nearest 0.01 for proton and 0.1 for carbon (reference: $CHCl_3$ [1H: 7.26 ppm, 13 C: 77.0 ppm]. Coupling constants J were reported in Hz to the nearest 0.01 Hz. Peak multiplicity was indicated as follows s (singlet), d (doublet), t (triplet), q (quartet), m (multiplet), br (broad signal) ad (apparent doublet) and aq (apparent quartet).[34] High resolution mass analyses were acquired with a resolution of 70000 FWHM at m/z = 200 in an alternate electrospray mode with data-dependent

Research Article
doi.org/10.1002/ejoc.202200769

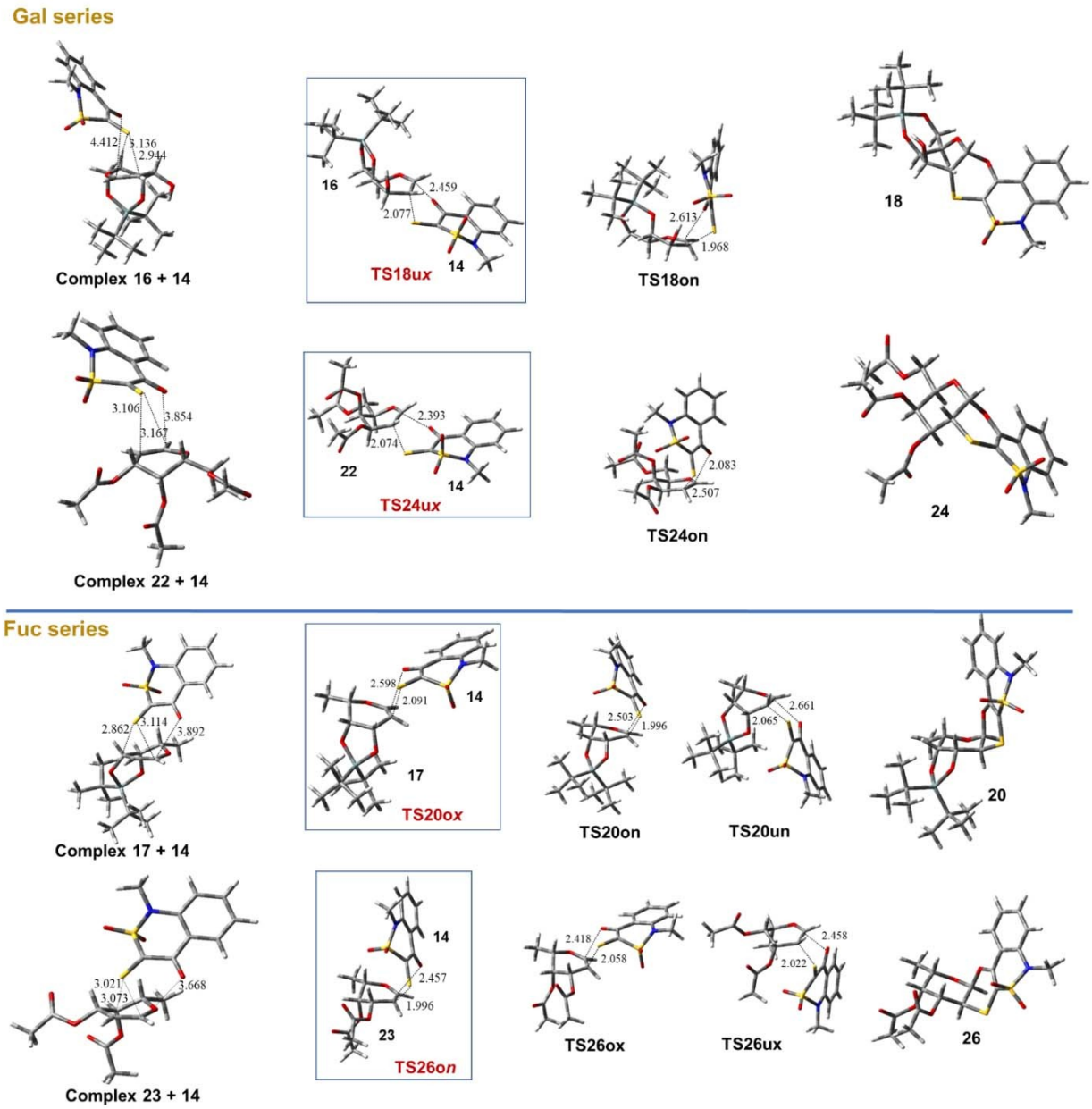

Figure 3. 3D-plots of the complexes, all the transition states (TSs) located for the ihDA of **14** with dienophiles **16**–**17** and **22**–**23** and of the cycloadducts **18**, **20**, **24** and **26**. 3D-plots of the most stable transition states (TSs) for the reaction of **14** with **16**–**22** (Gal series) and **17**–**23** (Fuc series) are TS18*ux*, TS24*ux*, TS20*ox*, TS26*on* (highlighted in the blue form). Displacement vectors for TS imaginary frequencies are shown as dotted lines and distances are reported in angstroms. (o = over, u = under, *x* = exo, *n* = endo).

acquisition of HCD fragmentation spectra (resolution 17500 FWHM at m/z = 200) of the more abundant monocharged ions (Q-Exactive hybrid quadrupole – orbitrap mass analyzer, Thermo Scientific).

Synthesis of 2-((1-methyl-4-hydroxy-2,2-dioxido-1*H*-benzo[c][1,2]thiazin-3-yl)thio)isoindoline-1,3-dione 12. To an ice-cooled solution of 1-methyl-1*H*-benzo[c][1,2]thiazin-4(3*H*)-one 2,2-dioxide **9** (200 mg, 0.95 mmol) in chloroform (1,1 mL) phthalimide-sulfenyl chloride **11** (200 mg, 0.78 mmol) was added under dark. The reaction mixture was stirred for 1 h, then 10 mL of cold hexane (5 mL) were added and the solid was recovered by filtration on Hirsh funnel. The solid was further washed with cold hexane (6 mL) to afford 276 (0.71 mmol) of **12** (75% yield) as a white solid, which is a mixture of ketone:enol tautomers in 1:5.5 ratio. ^{1}H-NMR (400 MHz, $CDCl_3$) δ: 10.17 (s, 1 H, OH enol form), 8.11–8.05 (m, 1H, Ar-thiazine), 7.98–7.92 (m, 2H, H-a′, H-a),7.84–7.79 (m, 2H, H-b′, H-b), 7.64–7.57 (m, 1H, Ar-Thiazine), 7.26–7.20 (m, 1H, Ar-thiazine), 7.18–7.13 (m, 1H, Ar-thiazine), 4.34 (s, 1H, H-3, H-α ketone) 3.51 (s, 3H, CH_3-N). ^{13}C-NMR (101 MHz, $CDCl_3$) δ: 166.79, 141.51, 135.14, 134.95, 127.83, 124.56, 124.33, 123.58, 122.72, 117.01, 116.28, 105.83, 31.29.

Synthesis of 2-((1-benzyl-4-hydroxy-2,2-dioxido-1H-benzo[c][1,2]thiazin-3-yl)thio)isoindoline-1,3-dione 13. To an ice cooled solution of 1-benzyl-1*H*-benzo[c][1,2]thiazin-4(3*H*)-one 2,2-dioxide **10** (156 mg, 0.81 mmol) in chloroform (2 mL) phthalimide-sulfenyl chloride **11** (191 mg, 0.9 mmol) was added under dark. The

Research Article
doi.org/10.1002/ejoc.202200769

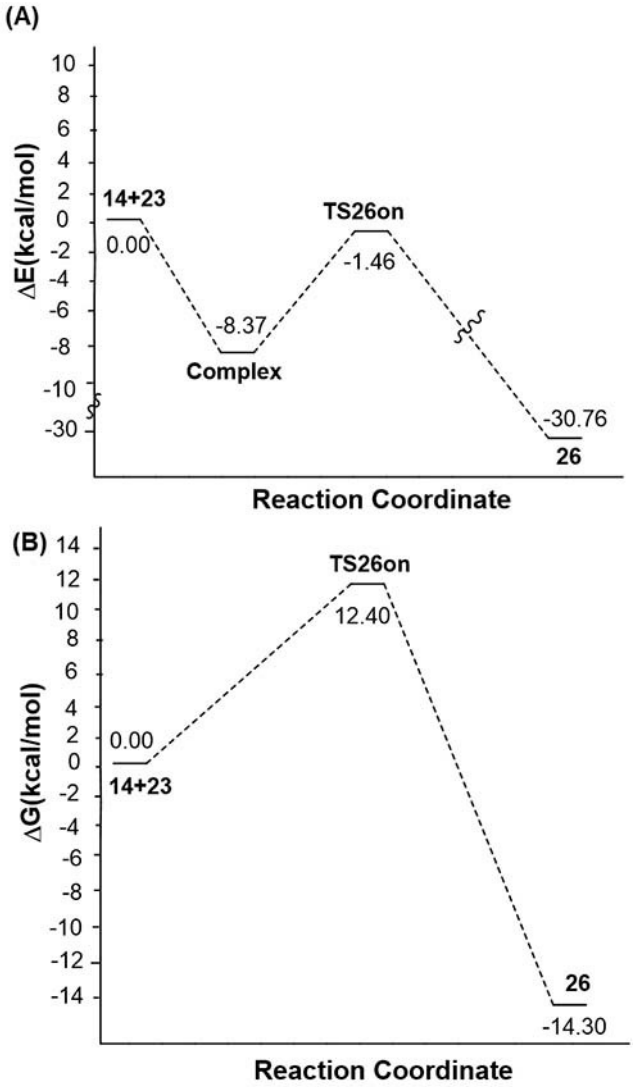

Figure 4. Energy (A) and free-energy (B) profiles determined for the favorite channel of the ihDA of the diene **14** with the dienophile **23**.

reaction mixture was stirred for 1 h, then 20 mL of cold hexane were added and the solid was recovered by filtration on Hirsh funnel. The solid was further washed with cold hexane (10 mL) to afford 206 mg (0.64 mmol) of **13** (79% yield) as a white solid, which is a mixture of ketone:enol tautomers in 1:1.7 ratio. ^{1}H-NMR (400 MHz, $CDCl_3$) δ : 10.13 (s, 1H, OH enol form), 8.07–8.02 (m, 1H, thiazine), 7.98–7.95 (m, 2H, H-a′, H-a), 7.84–7.79 (m, 2H, H-b′, H-b), 7.53–7.43 (m, 1H, Ar-thiazine), 7.36–7.12 (m, 8H, Ar-thiazine, CH_2—*Ph*), 5.18 (s, 2H, H-6, enol), 5.17 (s, 2H, H-6 ketone), 4.24 (s, 1H, H-α ketone). ^{13}C NMR (50 MHz, $CDCl_3$) δ: 166.90, 140.98, 136.40, 135.57, 135.16, 134.95, 134.18, 131.81, 131.65, 129.42, 129.07, 128.70, 127.79, 127.12, 126.47, 124.58, 124.35, 123.42, 118.80, 61.78, 51.45.

Synthesis of compound 18. In a sealed NMR tube **16** (13.5 mg, 0.047 mmol) was dissolved in $CDCl_3$, then pyridine (22 mg, 23 μL, 0.28 mmol) and **12** (11 mg, 0.028 mmol) were added and the mixture was warmed at 45 °C. Reaction mixture was monitored by 1H-NMR and by TLC. Then, two additional batches of **12** (11 mg, 0.028 mmol and 18 mg, 0.038 mmol respectively) were added each 24 h. After 72 h the reaction was concentrated to dryness. The crude was purified by flash chromatography on silica gel column (DCM : Acetone 100:1, $Rf = 0.3$) to afford 18 mg of **18** (73% yield) as glassy solid. $[\alpha]_D^{20} = +73$ ($c = 0.07$, $CHCl_3$).^{1}H-NMR (400 MHz, $CDCl_3$) δ: 7.72 (dd, $J = 7.9$ Hz, $J = 1.3$ Hz, 1H, Ar), 7.50–7.45 (m, 1H, Ar), 7.23–7.16 (m, 2H, Ar), 5.89 (d, $J_{1\text{-}2} = 2.9$ Hz, 1H, H-1), 4.51 (ad, $J =$ 2.8 Hz, 1H, H-4), 4.35-4.32 (m, 2H, H-6), 4.08–4.03 (m, 1H, H-5), 3.71 (dd, $J_{2\text{-}3} = 10.6$ Hz, $J_{23\text{-}4} = 3.0$ Hz, 1H, H-3), 3.61 (dd, $J_{3\text{-}2} = 10.6$ Hz, $J_{2\text{-}1} = 2.9$ Hz, 1H, H-2), 3.47 (s, 3H, CH_3–N), 1.084 (s, 9H, (tBu)$_2$Si), 1.077 (s, 9H, (tBu)$_2$Si). ^{13}C-NMR (101 MHz, $CDCl_3$) δ: 148.35, 138.39, 130.93, 123.31, 123.24, 118.93, 117.20, 104.28, 96.89, 72.28, 69.81, 66.74, 66.43, 40.15, 31.81, 27.54, 27.27, 23.35, 20.82. HRMS (ESI): *m/z* calcd for $C_{23}H_{33}NO_7S_2Si + H^+$ 528.1540 $[M+H]^+$, found 528.1540.

Synthesis of compound 19. In a sealed NMR tube **16** (13.5 mg, 0.047 mmol) was dissolved in $CDCl_3$, then pyridine (22 mg, 23 μL, 0.28 mmol) and **13** (13 mg, 0.028 mmol) were added and the mixture warmed at 45 °C. Reaction mixture was monitored by 1H-NMR and by TLC. Then, two additional batches of **13** (13 mg, 0.028 mmol and 18 mg, 0.038 mmol respectively) were added each 24 h. After 72 h the reaction was concentrated to dryness. The crude was purified by flash chromatography on silica gel column (DCM : Acetone 40:1, $Rf = 0.5$) to afford 17.3 mg of **19** (74% yield) as glassy solid. $[\alpha]_D^{20} = +47$ ($c = 0.3$, $CHCl_3$). ^{1}H-NMR (400 MHz, $CDCl_3$) δ: 7.65 (dd, $J = 8.0$ Hz, $J = 1.4$ Hz, Ar), 7.38–7.33 (m, 1H, Ar), 7.32–7.16 (m, 8H, Ar), 5.81 (d, $J_{2\text{-}1} = 2.7$ Hz, 1H, H1), 5.09 (A_2 system, 2H, CH_2-Ph), 4.46 (ad, $J = 4$ Hz, 1H, H-4), 4.32–4.29 (m 2H, H-6), 4.01–3.97 (m, 1H, H-5), 3.60 (dd, $J_{2\text{-}3} = 10.6$ Hz, $J_{2\text{-}1} = 2.7$ Hz, 1H, H-2), 3.52 (dd, $J_{3\text{-}2} = 10.6$ Hz, $J_{3\text{-}4} = 2.9$ Hz, 1H, H-3), 1.08 (s, 18H, (tBu)$_2$Si). ^{13}C-NMR (101 MHz, $CDCl_3$) δ: 148.01, 137.49, 135.32, 130.57, 128.62, 127.88, 127.57, 124.23, 123.35, 120.81, 120.35, 105.67, 96.68, 72.31, 69.75, 66.71, 66.47, 52.48, 40.37, 27.55, 27.27, 23.35, 20.83. HRMS (ESI): *m/z*: calcd for $C_{29}H_{37}NO_7S_2Si + H^+$ 604.1854 $[M+H]^+$, found 604.1860.

Synthesis of compound 20. In a sealed NMR tube **17** (13 mg, 0.047 mmol) was dissolved in $CDCl_3$ (600 μL), then pyridine (22 mg, 23 μL, 0.28 mmol) and **12** (11 mg, 0.028 mmol) were added and the mixture was warmed at 45 °C. Reaction mixture was monitored by 1H-NMR and by TLC. Then, two additional batches of **12** (11 mg, 0.028 mmol and 18 mg, 0.038 mmol respectively) were added each 24 h. After 72 h the reaction was concentrated to dryness. The crude was purified by flash chromatography on silica gel column (DCM : Acetone 100:1, $Rf = 0.2$) to afford 18 mg of **20** (95% yield) as glassy solid. $[\alpha]_D^{20} = -74$ ($c = 0.57$, $CHCl_3$). ^{1}H-NMR (400 MHz, $CDCl_3$) δ: 7.81–7.75 (m, 1H, Ar), 7.52–7.46 (m, 1H, Ar), 7.25–7.20 (m, 1H, Ar), 7.20–7.16 (m, 1H, Ar), 5.90 (d, $J_{1\text{-}2} = 3.0$ Hz, 1H, H-1), 4.31 (ad, $J = 1.9$ Hz, 1H, H-4), 4.21 (aq, $J = 6.3$ Hz, 1H, H-5), 3.77 (dd, $J_{3\text{-}2} =$ 10.9 Hz, $J_{3\text{-}4} = 2.5$ Hz, 1H, H-3), 3.69 (dd, $J_{2\text{-}3} = 10.9$ Hz, $J_{2\text{-}1} = 3.1$ Hz, 1H, H-2), 3.46 (s, 3H, CH_3-N), 1.44 (t, $J = 10.2$ Hz, 3H, H-6), 1.068 (s, 9 H, tBu$_2$Si), 1.059 (s, 9 H, tBu$_2$Si). ^{13}C-NMR (101 MHz, $CDCl_3$) δ: 150.08, 138.45, 134.28, 131.21, 123.56, 123.54, 123.31, 118.68, 117.00, 101.88, 97.64, 73.34, 70.47, 66.35, 39.28, 31.48, 30.91, 27.87, 27.69, 21.38, 20.69, 17.19. HRMS (ESI) *m/z*: calcd for $C_{23}H_{33}NO_6S_2Si + H^+$ 512.1591 $[M+H^+]$, found 512.1591.

Synthesis of compound 21. In a sealed NMR tube **17** (13 mg, 0.047 mmol) was dissolved in $CDCl_3$, then pyridine (22 mg, 23 μL, 0.28 mmol) and **13** (13 mg, 0.028 mmol) were added and the mixture was warmed at 45 °C. Reaction mixture was monitored by 1H-NMR and by TLC. Then, two additional batch of **13** (13 mg, 0.028 mmol and 15 mg, 0.038 mmol respectively) were added each 24 h. After 72 h the reaction was concentrated to dryness. The crude was purified by flash chromatography on silica gel column (DCM : Acetone 100:1, $Rf = 0.5$) to afford 15.3 mg of **21** (74% yield) as glassy solid. $[\alpha]_D^{20} = -53$ ($c = 0.196$, $CHCl_3$). ^{1}H-NMR (400 MHz, $CDCl_3$) δ: 7.74–7.70 (m, 1H, Ar), 7.40–7.35(m, 1H, Ar), 7.32–7.18 (m, 8H, Ar), 5.82 (d, $J_{1\text{-}2} = 3.0$ Hz, 1H, H-1), 5.15–5.10 (A part of an AB, $J_{AB} = 16.4$ Hz, 1H, CH_2-Ph), 5.09–5.05 (B part of an AB, $J_{AB} = 16.4$ Hz,

1H, CH_2-Ph), 4.26 (ad, $J=2.2$ Hz, 1H, H-4), 4.15 (aq, $J=6.4$ Hz, 1H, H-5), 3.68 (dd, $J_{2\text{-}3}=10.9$ Hz, $J_{2\text{-}1}=3.1$ Hz, 1H, H-2), 3.57 (dd, $J_{3\text{-}2}=10.9$ Hz, $J_{3\text{-}4}=2.5$ Hz, 1H, H-3), 1.41 (d, $J_{6\text{-}5}=6.4$ Hz, 3H, H-6), 1.07 (s, 9H, $(t\text{Bu})_2$Si), 1.06 (s, 9H, $(t\text{Bu})_2$Si). ^{13}C-NMR (101 MHz, $CDCl_3$) δ: 149.76, 137.56, 135.24, 134.35, 130.98, 128.65, 127.96, 127.43, 124.31, 123.62, 123.58, 120.48, 120.09, 102.98, 97.30, 73.16, 70.44, 66.36, 52.01, 39.32, 27.86, 27.71, 21.40, 20.71, 17.20. HRMS (ESI): *m/z* calcd for $C_{29}H_{37}NO_6S_2Si+H^+$ 588.1904 $[M+H]^+$, found 588.1897.

Synthesis of compound 24. In a sealed NMR tube **22** (13 mg, 0.047 mmol) was dissolved in $CDCl_3$, then pyridine (22 mg, 23 μL, 0.28 mmol) and **12** (11 mg, 0.028 mmol) were added and the mixture was warmed at 45 °C. Reaction mixture was monitored by 1H-NMR and by TLC. Then, after 24, 48, 72 and 168 h four batch of **12** (11 mg 0.028 mmol, 15 mg 0.038 mmol, 11 mg 0.028 mmol and 18 mg 0.047 mmol respectively) were added. After 192 h the reaction was concentrated to dryness. The crude was purified by flash chromatography on silica gel column (petroleum ether:Ethyl acetate 3:1, *Rf*=0.4) to afford 18.2 mg of **24** (37% yield) as glassy solid. $[\alpha]_D^{20}=+103$ ($c=0.51$, $CHCl_3$).[1]H-NMR (400 MHz, $CDCl_3$) δ: 7.77 (ad, $J=7.9$ Hz, 1H, Ar), 7.49 (at, $J=7.8$ Hz, 1H, Ar), 7.32–7.18 (m, 2H, Ar), 5.93 (d, $J_{1\text{-}2}=2.7$ Hz, 1H, H-1), 5.45 (ad, $J=2.7$ Hz, 1H, H-4), 5.07 (dd, $J_{3\text{-}2}=11.6$ Hz, $J_{3\text{-}4}=3.0$ Hz, 1H, H-3), 4.53–4.47 (m, 1H, H-6), 4.23–4.16 (m, 2H, H-5, H-6), 3.81 (dd, $J_{2\text{-}3}=11.6$ Hz, $J_{2\text{-}1}=2.7$ Hz, 1H, H-2), 3.44 (s, 3H, Me–N), 2.18 (s, 3H, Ac), 2.07 (s, 3H, Ac), 2.04 (s, 3H, Ac). ^{13}C-NMR (101 MHz, $CDCl_3$) δ: 170.30, 169.76, 169.54, 147.75, 138.54, 131.13, 123.68, 123.52, 119.05, 117.94, 104.29, 96.22, 69.06, 67.02, 65.82, 61.18, 36.94, 32.76, 20.67, 20.58, 20.52. HRMS (ESI): *m/z* calcd for $C_{21}H_{23}NO_{10}S_2+H^+$ 514,0836$[M+H]^+$, found 514.0836.

Synthesis of compound 25. In a sealed NMR tube **22** (13 mg, 0.047 mmol) was dissolved in $CDCl_3$, then pyridine (22 mg, 23 μL, 0.28 mmol) and **13** (13 mg, 0.028 mmol) were added and the mixture was warmed at 45 °C. Reaction mixture was monitored by 1H-NMR and by TLC. Then, after 24, 48, 72 and 168 h four batch of **13** (13 mg 0.028 mmol, 18 mg 0.038 mmol, 13 mg 0.028 mmol and 22 mg 0.047 mmol respectively) were added. After 192 h the reaction was concentrated to dryness. The crude was purified by flash chromatography on silica gel column (petroleum ether : ethyl acetate 3:1, *Rf*=0.3) to afford 11.6 mg of **25** (38% yield) as glassy solid. $[\alpha]_D^{20}=+132$ ($c=0.13$, $CHCl_3$).[1]H-NMR (400 MHz, $CDCl_3$) δ: 7.73 (dd, $J=8.0$, 1.5 Hz, 1H, Ar), 7.41–7.20 (m, 7H, Ar), 7.15 (d, $J=7.7$ Hz, 1H, Ar), 5.89 (d, $J_{1\text{-}2}=2.7$ Hz, 1H, H-1), 5.47 (m, 1H, H-4), 5.18–5.12 (A part of an AB system, $J_{AB}=16.5$ Hz, 1H, CH_2–Ph), 5.09 (dd, $J_{3\text{-}2}=11.6$ Hz, $J_{3\text{-}4}=3.0$ Hz, 1H, H-3), 5.03–4.99 (B part of an AB system, $J_{AB}=16.5$ Hz, 1H, CH_2–Ph), 4.50 (at, $J=6.8$ Hz, 1H, H-5), 4.24-4.20 (A part of an ABX system $J_{AB}=11.6$ Hz, $J_{AX}=6.4$ Hz, 1H, H-6), 4.19-4.16 (B part of an ABX system, $J_{BA}=11.6$ Hz, $J_{BX}=7.2$ Hz, 1H, H-6), 3.82 (dd, $J_{2\text{-}3}=11.6$ Hz, $J_{2\text{-}1}=2.8$ Hz, 1H, H-2), 2.19 (s. 3H, Ac) 2.07 (s, 3H, Ac), 2.06 (s, 3H, Ac). ^{13}C-NMR (101 MHz, $CDCl_3$) δ: 170.30, 169.76, 169.50, 147.66, 137.67, 135.63, 130.83, 128.77, 127.86, 127.21, 124.18, 123.52, 120.12, 119.82, 105.34, 96.15, 69.08, 67.05, 65.89, 61.18, 52.28, 37.11, 20.67, 20.59, 20.54. HRMS (ESI): *m/z* calcd for $C_{27}H_{27}NO_{10}S_2+H^+$ 590.1146 $[M+H]^+$, found 590.1149.

Synthesis of compound 26. In a sealed NMR tube **23** (10 mg, 0.047 mmol) was dissolved in $CDCl_3$, then pyridine (22 mg, 23 μL, 0.28 mmol) and **12** (11 mg, 0.028 mmol) were added and the mixture was warmed at 45 °C. Reaction mixture was monitored by 1H-NMR and by TLC. Then, two additional batch of **12** (11 mg, 0.028 mmol and 15 mg, 0.038 mmol respectively) were added each 24 h. After 72 h the reaction was concentrated to dryness. The crude was purified by flash chromatography on silica gel column (DCM : Acetone 100:1, *Rf*=0.3) to afford 16.6 mg of **26** (78% yield) as glassy solid. $[\alpha]_D^{20}=-168$ ($c=0.57$, $CHCl_3$).[1]H NMR (400 MHz, $CDCl_3$) δ: 7.82–7.84 (m, 1H, Ar), 7.58–7.44 (m, 1H, Ar), 7.31–7.16 (m, 7H), 5.90 (d, $J_{1\text{-}2}=2.8$ Hz, 1H, H-1), 5.29 (ad, $J=2.2$ Hz, 1H, H-4), 5.07 (dd, $J_{3\text{-}2}=11.6$ Hz, $J_{3\text{-}4}=3.0$ Hz, 1H, H-3), 4.43 (aq, $J=6.5$ Hz, 1H, H-5), 3.79 (dd, $J_{2\text{-}3}=11.6$ Hz,$J_{2\text{-}1}=2.8$ Hz, 1H, H-2), 3.44 (s, 3H, CH_3–N), 2.20 (s, 3H, Ac), 2.04 (s, 3H, Ac), 1.25 (d, $J=6.5$ Hz, 3H, H-6). ^{13}C-NMR (101 MHz, $CDCl_3$) δ: 170.16, 169.62, 147.93, 138.54, 131.02, 123.58, 119.19, 117.91, 104.18, 96.50, 70.22, 67.61, 66.32, 36.89, 32.75, 20.59, 16.12. HRMS (ESI): *m/z* calcd for $C_{19}H_{21}NO_8S_2+H^+$ 456.0781 $[M+H]^+$, found 456.0779.

Synthesis of compound 27. In a sealed NMR tube **23** (10 mg, 0.047 mmol) was dissolved in $CDCl_3$, then pyridine (22 mg, 23 μL, 0.28 mmol) and **13** (13 mg, 0.028 mmol) were added and the mixture was warmed at 45 °C. Reaction mixture was monitored by 1H-NMR and by TLC. Then, after 24 h and 48 h two additional batch of **13** (13 mg, 0.028 mmol and 18 mg, 0.038 mmol respectively) were added. After 72 h the reaction was concentrated to dryness. The crude was purified by flash chromatography on silica gel column (DCM : Acetone 100:1, Rf=0.5) to afford 15.3 mg of **27** (62% yield) as glassy solid. $[\alpha]_D^{20}=-110$ ($c=0.22$, $CHCl_3$). ^{1}H-NMR (400 MHz, $CDCl_3$) δ: 7.76–7.72 (m, 1H, Ar), 7.39–7.24 (m, 5H, Bn), 7.22 (m, 1H, Ar), 7.14 (m, 1H, Ar), 5.85 (d, $J=2.7$ Hz, 1H, H-1), 5.34–5.26 (m, 1H, H-4), 5.19–5.12 (A part of an AB system, $J=16.5$ Hz, 1H, CH_2-Ph), 5.09 (dd, $J_{3\text{-}2}=11.6$ Hz, $J_{3\text{-}4}$ 3.0 Hz, 1H, H-3), 5.04–4.97 (B part of an AB system, $J=16.5$ Hz, 1H, CH_2–Ph), 4.43 (aq, $J=6.5$ Hz, 1H, H-5), 3.80 (dd, $J_{2\text{-}3}=11.6$ Hz, $J_{2\text{-}1}=2.7$ Hz, 1H, H-2), 2.21 (s, 3H, Ac), 2.07 (s, 3H, Ac), 1.25 (d, $J=6.5$ Hz, 3H, H-6). ^{13}C-NMR (101 MHz, $CDCl_3$) δ: 170.22, 169.65, 147.83, 137.62, 135.68, 130.75, 130.03, 128.77, 127.84, 127.20, 124.10, 123.59, 120.22, 119.75, 114.32, 105.18, 96.39, 70.22, 67.62, 66.41, 52.26, 37.02, 20.66, 20.64, 16.13. HRMS (ESI): *m/z* calcd for $C_{25}H_{25}NO_8S_2+H^+$ 532.1093 $[M+H]^+$, found 532.1094.

General procedure for deacetylation reaction. To a stirred solution of **24**–**27** (0.05 M) in methanol, anhydrous potassium carbonate (0.3 eq) was added and the mixture was stirred at room temperature for 1 h. Then, the reaction mixture was dried under reduced pressure and the crude was purified by filtration on silica gel (Ethyl acetate). **Compound 5**: (80% yield), glassy solid. $[\alpha]_D^{20}=+38$ ($c=0.29$, $CHCl_3$).[1]H NMR (400 MHz, CD_3OD) δ: 7.85 (dd, $J=8.0$, $J=1.4$ Hz, 1H, Ar), 7.60–7.45 (m, 1H, Ar), 7.35 (ad, $J=8.2$ Hz, 1H, Ar), 7.27 (at, $J=7.7$ Hz, 1H, Ar), 5.95 (d, $J_{1\text{-}2}=2.9$ Hz, 1H, H-1), 4.15–4.08 (m, 1H, H-5), 3.95 (d, $J=2.1$ Hz, 1H, H-4), 3.88–3.83 (A part of an ABX system, $J_{A\text{-}B}=11.5$ Hz, $J_{A\text{-}X}=6.9$ Hz, 1H, H-6a), 3.79–3.75 (B part of an ABX system, $J_{B\text{-}A}=11.5$ Hz, $J_{B\text{-}X}=5.0$ Hz, 1H), 3.68 (dd, $J_{3\text{-}2}=10.9$ Hz, $J_{3\text{-}4}=2.9$ Hz, 1H, H-3), 3.63 (dd, $J_{2\text{-}3}=10.9$ Hz, $J_{2\text{-}1}=2.8$ Hz, 1H, H-2), 3.42 (s, 3H, Me–N). ^{13}C NMR (101 MHz, CD_3OD) δ: 149.11, 138.52, 130.75, 123.19, 123.05, 122.94, 119.71, 119.06, 117.37, 97.48, 73.98, 69.00, 65.67, 61.32, 39.49, 30.63. HRMS (ESI): m/z calcd for $C_{15}H_{17}NO_7S_2+H^+$: 388.0519 $[M+H]^+$; found: 388.0517. FT-IR ν^-: 3744 (s, OH, stretching), 3590 (bs, OH stretching), 3032 (s, CH stretching), 2930 (bs, CH), 1742, 1691, 1648 (s, C=C stretching), 1607, 1552, 1531, 1325 (s, SO, stretching) and 1092 cm^{-1} (s, C–O-C stretching). **Compound 6**: (95% yield), glassy solid. $[\alpha]_D^{20}=+32$ ($c=0.35$, $CHCl_3$). ^{1}H NMR (400 MHz, CD_3OD) δ: 7.75 (dd, $J=8.0$ Hz, $J=1.3$ Hz, 1H, Ar), 7.44–7.38 (m, 1H, Ar), 7.34 (d, $J=7.4$ Hz, 1H, Ar), 7.30–7.21 (m, 6H, Ar), 5.81 (d, $J_{1\text{-}2}=3.0$ Hz, 1H, H-1), 5.16–5.12 (A part of an AB system, $J_{A\text{-}B}=16.2$ Hz, 1H, CH_2-Ph), 5.10–5.06 (B part of an AB system, $J_{B\text{-}A}=16.2$ Hz, 1H, CH_2-Ph), 4.11–4.01 (m, 1H, H-5), 3.93 (ad, $J=2.6$ Hz, 1H, H-4), 3.86–3.81 (A part of an ABX system, $J_{A\text{-}B}=11.5$ Hz, $J_{B\text{-}X}=6.9$ Hz, 1H), 3.77–3.73 (B part of an ABX system, $J_{B\text{-}A}=11.5$ Hz, $J_{B\text{-}X}=5.0$ Hz, 1H, H-6_b), 3.67 (dd, $J_{2\text{-}3}=10.9$ Hz, $J_{2\text{-}1}=3.0$ Hz, 1H, H-2), 3.55 (dd, $J_{3\text{-}2}=10.9$ Hz, $J_{3\text{-}4}=3.0$ Hz, 1H, H-3). ^{13}C NMR (101 MHz, CD_3OD) δ 148.61, 137.20, 135.42, 130.23, 128.10, 127.49, 127.42, 124.14, 123.03, 121.19, 120.52, 97.06, 73.91, 68.95, 65.92, 61.29, 51.43, 39.69. HRMS (ESI): m/z calcd for $C_{21}H_{21}NO_7S_2+H^+$: 464.0832 $[M+H]^+$; found: 464.0836. FT-IR ν^-: 3566, 3030 (s, CH stretching) 3010 (s, CH stretching) 2928 (bs, CH stretching), 1603, 1335 (s, SO stretching) 1233 (s, C–O-C stretching), 1168 and 1092 cm^{-1}(s, C–O–C stretching). **Compound 7**: (80% yield), glassy

solid. $[\alpha]_D^{20} = -115$ ($c = 0.48$, $CHCl_3$) ^{1}H NMR (400 MHz, $CDCl_3$) δ 7.78 (dd, $J = 8.0$ Hz, 1.3 Hz, Ar), 7.52–7.45 (m, 1H, Ar), 7.25–7.16 (m, 2H, Ar), 5.88 (d, $J_{1\text{-}2} = 3.1$ Hz, 1H, H-1), 4.22 (aq, $J = 6.6$ Hz, 1H, H-5), 3.87 (as, 1H, H-4), 3.75 (dd, $J_{3\text{-}2} = 10.5$ Hz, $J_{3\text{-}4} = 2.8$ Hz, 1H, H-3), 3.64 (dd, $J_{2\text{-}3} = 10.5$ Hz, $J_{2\text{-}1} = 3.1$ Hz, 1H, H-2), 3.45 (s, 3H, CH_3–N), 2.79 (s, 1H, OH), 1.81 (s, 1H, OH), 1.43 (d, $J_{6\text{-}5} = 6.55$ Hz, 3H, H-6).^{13}C NMR (101 MHz, $CDCl_3$) δ 149.88, 138.38, 131.20, 123.52, 123.36, 118.75, 117.04, 102.20, 97.35, 70.88, 69.03, 65.74, 39.12, 31.53, 16.39. HRMS (ESI): m/z calcd for $C_{15}H_{17}NO_6S_2 + H^+$: 372.0570 $[M+H]^+$; found: 372.0575. FT-IR ν$^-$: 3588 (bs, OH, stretching), 3572, 3036 (s, CH stretching), 2912 (bs, CH stretching), 1738, 1605, 1321 (s, SO stretching), 1237 (s, C–O–C stretching), 1167 and 1092 cm^{-1} (s, C–O–C stretching). **Compound 8**: (94% yield), glassy solid. $[\alpha]_D^{20} = -78$ ($c = 0.41$, $CHCl_3$). ^{1}H NMR (200 MHz, $CDCl_3$) δ 7.73 (dd, $J = 8.2$ Hz, 1.6 Hz, 1H, Ar), 7.48–7.33 (m, 1H, Ar), 7.30–7.17 (m, 7H, Ar), 5.79 (d, $J_{1\text{-}2} = 2.6$ Hz, 1H, H-1), 5.09 (A_2 system, 2H, CH_2Ph), 4.17 (aq, $J = 6.6$ Hz, 1H, H-5), 3.84 (as, 1H,), 3.69–3.50 (m, 2H, H-3 and H-2), 3.16 (s, 1H, OH), 2.60 (s, 1H, OH), 1.42 (d, $J_{6\text{-}5} = 6.6$ Hz, 3H, H-6). ^{13}C NMR (50 MHz, $CDCl_3$) δ 149.50, 137.64, 135.27, 130.86, 128.60, 127.94, 127.50, 124.34, 123.55, 120.74, 120.26, 103.63, 96.97, 70.75, 68.95, 65.96, 52.26, 39.33, 16.32. HRMS (ESI): m/z calcd for $C_{21}H_{21}NO_6S_2 + H^+$: 448.0883 $[M+H]^+$; found: 448.0879. FT-IR ν$^-$: 3588 (bs, OH, stretching), 3020 (s, CH, stretching), 2918 (bs, CH, stretching), 1335 (s, SO stretching), 1226 (s, C–O–C stretching), 1165 and 1092 cm^{-1} (s, C–O–C stretching).

Computational Methods

All the calculations were carried out using the GAUSSIAN016 program package.[35] All the structures of reactants, transition states, and products were optimized in the gas-phase at the B3LYP/6-311 + G(2df,p) level for the S atom and 6-311 + G(d,p) level for the other atoms, to correctly describe the geometries and the electronic properties of compounds that contain a sulfur atom. The orientations of the acetyl groups in the dienophiles **22**–**23** are described through the torsion angles τ_1 [C(2)–C(3)–O–C(3′)], τ_2 [C(5)–C(4)–O–C(4′)], τ_3 [O–C(5)–C(5′)–C(O)], and τ_4 [C(5)–C(5′)–C-C(O)–C], and τ_1 [C(1)–C(6)–C(7)–C(8)] and τ_2 [C(7)–C(8)–C(9)–C(10)].The reaction pathways were confirmed by IRC analyses performed at the same level as above. Vibrational frequencies were computed at the same level of theory to define the optimized structures as minima or transition states, which present an imaginary frequency corresponding to the forming bonds. Thermodynamics at 298.15 K allowed the enthalpies and the Gibbs free energies to be calculated. The polar nature of the reactions has been evaluated through the analysis of the reactivity indices. The electronic chemical potential (μ), chemical hardness (η), global electrophilicity (ω), and global nucleophilicity (N), were computed at the same level as above.

Acknowledgements

Authors are very grateful to Prof. Ugo Chiacchio for helpful discussions. B.R. and G.B. thank COST action CA18103 INNOGLY: INNOvation with GLYcans: new frontiers from synthesis to new biological targets. B.R., G.B. and G.A. thank MIUR-Italy ("Progetto Dipartimenti di Eccellenza 2018–2022" allocated to Department of Chemistry "Ugo Schiff"). B.R. and G.B. thank Fondazione Umberto Veronesi for supporting the postdoctoral fellowship 2022 of G.B. Open Access funding provided by Università degli Studi di Firenze within the CRUI-CARE Agreement.

Conflict of Interest

The authors declare no conflict of interest.

Data Availability Statement

The data that support the findings of this study are available from the corresponding author upon reasonable request.

Keywords: Benzo[*c*][1,2]thiazine · Glycomimetics · Heterodienes · Diels-Alder reaction · Synthetic methods

[1] a) B. Ernst, J. L. Magnani, *Nat. Rev. Drug Discovery* **2009**, *8*, 661–677; b) P. Compain, *Molecules* **2018**, *23*, 1658.
[2] a) A. Bernardi, J. Jiménez-Barbero, A. Casnati, C. De Castro, T. Darbre, F. Fieschi, J. Finne, H. Funken, K.-E. Jaeger, M. Lahmann, T. K. Lindhorst, M. Marradi, P. Messner, A. Molinaro, P. V. Murphy, C. Nativi, S. Oscarson, S. Penadés, F. Peri, R. J. Pieters, O. Renaudet, J.-L. Reymond, B. Richichi, J. Rojo, F. Sansone, C. Schäffer, W. B. Turnbull, T. Velasco-Torrijos, S. Vidal, S. Vincent, T. Wennekes, H. Zuilhof, A. Imberty, *Chem. Soc. Rev.* **2013**, *42*, 4709–4727; b) S. Cecioni, A. Imberty, S. Vidal, *Chem. Rev.* **2015**, *115*, 525–561.
[3] C. U. Kim, W. Lew, M. A. Williams, H. Liu, L. Zhang, S. Swaminathan, N. Bischofberger, M. S. Chen, D. B. Mendel, C. Y. Tai, W. G. Laver, R. C. Stevens, *J. Am. Chem. Soc.* **1997**, *119*, 681–690.
[4] M. von Itzstein, W. Y. Wu, G. B. Kok, M. S. Pegg, J. C. Dyason, B. Jin, T. Van Phan, M. L. Smythe, H. F. White, S. W. Oliver, *Nature* **1993**, *363*, 418–423.
[5] X. Chen, Y. Zheng, Y. Shen, *Curr. Med. Chem.* **2006**, *13*, 109–116.
[6] L. K. Campbell, D. E. Baker, R. K. Campbell, *Ann. Pharmacother.* **2000**, *34*, 1291–1301.
[7] N. J. Weinreb, J. A. Barranger, J. Charrow, G. A. Grabowski, H. J. Mankin, P. Mistry, *Am. J. Hematol.* **2005**, *80*, 223–229.
[8] B. E. Maryanoff, S. O. Nortey, J. F. Gardocki, R. P. Shank, S. P. Dodgson, *J. Med. Chem.* **1987**, *30*, 880–887.
[9] E. Braunwald, *N. Engl. J. Med.* **2022**, *386*, 2024–2034.
[10] E. Bokor, S. Kun, D. Goyard, M. Tóth, J.-P. Praly, S. Vidal, L. Somsák, *Chem. Rev.* **2017**, *117*, 1687–1764.
[11] a) M. Meanwell, G. Fehr, W. Ren, B. Adluri, V. Rose, J. Lehmann, S. M. Silverman, R. Rowshanpour, C. Adamson, M. Bergeron-Brlek, H. Foy, V. R. Challa, L.-C. Campeau, T. Dudding, R. Britton, *Commun. Chem.* **2021**, *4*, 96; b) A. Tamburrini, C. Colombo, A. Bernardi, *Med. Res. Rev.* **2020**, *40*, 495–531; c) A. Bernardi, S. Sattin, *Eur. J. Org. Chem.* **2020**, *30*, 4652–4663.
[12] a) M. Cacciarini, S. Menichetti, C. Nativi, B. Richichi, *Curr. Org. Synth.* **2007**, *4*, 47–57; b) G. Gabrielli, F. Melani, S. Bernasconi, C. Lunghi, B. Richichi, P. Rollin, C. Venturi, C. Nativi, *J. Carbohydr. Chem.* **2009**, *28*, 124–141.
[13] a) B. Richichi, A. Imberty, E. Gillon, R. Bosco, I. Sutkeviciute, F. Fieschi, C. Nativi, *Org. Biomol. Chem.* **2013**, *11*, 4086–4094; b) B. Richichi, J. McKimm-Breschkin, V. Baldoneschi, C. Nativi, *Arkivoc* **2013**, *2014*, 65–79; c) B. Richichi, B. Thomas, M. Fiore, R. Bosco, H. Qureshi, C. Nativi, O. Renaudet, L. A. BenMohamed, *Angew. Chem. Int. Ed.* **2014**, *53*, 11917–11920; *Angew. Chem.* **2014**, *126*, 12111–12114; d) A. Arcangeli, L. Toma, L. Contiero, O. Crociani, L. Legnani, C. Lunghi, E. Nesti, G. Moneti, B. Richichi, C. Nativi, *Bioconjugate Chem.* **2010**, *21*, 1432–1438.
[14] D. Goyard, V. Baldoneschi, A. Varrot, M. Fiore, A. Imberty, B. Richichi, O. Renaudet, C. Nativi, *Bioconjugate Chem.* **2018**, *29*, 83–88.
[15] K. C. Martin, J. Tricomi, F. Corzana, A. García-García, L. Ceballos-Laita, T. Hicks, S. Monaco, J. Angulo, R. Hurtado-Guerrero, B. Richichi, R. Sackstein, *Chem. Commun.* **2021**, *57*, 1145–1148.
[16] M. Manuelli, S. Fallarini, G. Lombardi, C. Sangregorio, C. Nativi, B. Richichi, *Nanoscale* **2014**, *6*, 7643–7655.
[17] B. Richichi, G. Comito, L. Cerofolini, G. Gabrielli, A. Marra, L. Moni, A. Pace, L. Pasquato, P. Chiarugi, A. Dondoni, L. Toma, C. Nativi, *Bioorg. Med. Chem.* **2013**, *21*, 2756–2763.
[18] R. Ribeiro-Viana, E. Bonechi, J. Rojo, C. Ballerini, G. Comito, B. Richichi, C. Nativi, *Beilstein J. Org. Chem.* **2014**, *10*, 1317–1324.

[19] P. Arosio, G. Comito, F. Orsini, A. Lascialfari, P. Chiarugi, C. Ménard-Moyon, C. Nativi, B. Richichi, *Org. Biomol. Chem.* **2018**, *16*, 6086–6095.
[20] J. M. Herbert, *Comprehensive Heterocyclic Chemistry III*, Elsevier **2008**; pp 977–1092.
[21] Y. Volovenko, T. Volovnenko, K. Popov, *J. Heterocycl. Chem.* **2007**, *44*, 1413–1419.
[22] V. Gupta, K. S. Carroll, *Chem. Sci.* **2016**, *7*, 400–415.
[23] G. Capozzi, S. Menichetti, C. Nativi, A. Rosi, R. W. Franck, *Tetrahedron Lett.* **1993**, *34*, 4253–4256.
[24] J. Jiménez-Barbero, E. Dragoni, C. Venturi, F. Nannucci, A. Ardá, M. Fontanella, S. André, F. J. Cañada, H.-J. Gabius, C. Nativi, *Chem. Eur. J.* **2009**, *15*, 10423–10431.
[25] H. Grugel, F. Albrecht, M. M. K. Boysen, *Adv. Synth. Catal.* **2014**, *356*, 3289–3294.
[26] S. Zhang, Y.-H. Niu, X.-S. Ye, *Org. Lett.* **2017**, *19*, 3608–3611.
[27] a) L. Legnani, A. Porta, P. Caramella, L. Toma, G. Zanoni, G. Vidari, *J. Org. Chem.* **2015**, *80*, 3092–3100; b) V. Amendola, G. Bergamaschi, M. Boiocchi, L. Legnani, E. Lo Presti, A. Miljkovic, E. Monzani, F. Pancotti, *Chem. Commun.* **2016**, *52*, 10910–10913; c) P. Merino, M. A. Chiacchio, L. Legnani, I. Delso, T. Tejero, *Org. Chem. Front.* **2017**, *4*, 1541–1554; d) L. Legnani, R. Puglisi, A. Pappalardo, M. A. Chiacchio, G. Trusso Sfrazzetto, *Chem. Commun.* **2020**, *56*, 539–542.
[28] L. Legnani, C. Lunghi, F. M. Albini, C. Nativi, B. Richichi, L. Toma, *Eur. J. Org. Chem.* **2007**, *21*, 3547–3554.
[29] B. L. Oliveira, Z. Guo, G. J. L. Bernardes, *Chem. Soc. Rev.* **2017**, *46*, 4895–4950.
[30] L. R. Domingo, E. Chamorro, P. Pérez, *J. Org. Chem.* **2008**, *73*, 4615–4624.
[31] E. Chamorro, P. Pérez, L. R. Domingo, *Chem. Phys. Lett.* **2013**, *582*, 141–143.
[32] P. Pérez, L. R. Domingo, M. José Aurell, R. Contreras, *Tetrahedron* **2003**, *59*, 3117–3125.
[33] S. Badshah, A. Naeem, *Molecules* **2016**, *21*, 1054.
[34] P. J. Stevenson, *Org. Biomol. Chem.* **2011**, *9*, 2078–2084.
[35] Gaussian 16, Revision C.01, M. J. Frisch, G. W. Trucks, H. B. Schlegel, G. E. Scuseria, M. A. Robb, J. R. Cheeseman, G. Scalmani, V. Barone, G. A. Petersson, H. Nakatsuji, X. Li, M. Caricato, A. V. Marenich, J. Bloino, B. G. Janesko, R. Gomperts, B. Mennucci, H. P. Hratchian, J. V. Ortiz, A. F. Izmaylov, J. L. Sonnenberg, D. Williams-Young, F. Ding, F. Lipparini, F. Egidi, J. Goings, B. Peng, A. Petrone, T. Henderson, D. Ranasinghe, V. G. Zakrzewski, J. Gao, N. Rega, G. Zheng, W. Liang, M. Hada, M. Ehara, K. Toyota, R. Fukuda, J. Hasegawa, M. Ishida, T. Nakajima, Y. Honda, O. Kitao, H. Nakai, T. Vreven, K. Throssell, J. A. Montgomery, Jr., J. E. Peralta, F. Ogliaro, M. J. Bearpark, J. J. Heyd, E. N. Brothers, K. N. Kudin, V. N. Staroverov, T. A. Keith, R. Kobayashi, J. Normand, K. Raghavachari, A. P. Rendell, J. C. Burant, S. S. Iyengar, J. Tomasi, M. Cossi, J. M. Millam, M. Klene, C. Adamo, R. Cammi, J. W. Ochterski, R. L. Martin, K. Morokuma, O. Farkas, J. B. Foresman, D. J. Fox, Gaussian, Inc., Wallingford CT, **2016**.

Manuscript received: June 27, 2022
Revised manuscript received: September 23, 2022
Accepted manuscript online: September 27, 2022